

POSITRON DISTRIBUTION IN THE INNER GALACTIC RIDGE

R.L. Kinzer¹, W. R. Purcell², J.D. Kurfess¹

ABSTRACT

OSSE was used to measure the longitude and latitude distribution of positron annihilation in the inner galactic ridge using differential measurements relative to intensities at latitudes of $\pm 10^\circ$. An improved understanding of the 50 keV to 10 MeV continua has recently permitted accurate determinations of the positronium continuum flux intensities; this provides an ~ 5 times greater signal than was available in previous analyses which used only the 511 keV annihilation line. Within the statistical precision of the measurements, the line and positronium continuum components show indistinguishable distributions in both latitude and longitude. A differential measurement of their latitude distributions near the center indicates a narrow Gaussian ridge of $\sim 4.4^\circ$ FWHM. The longitude distribution of the ridge intensity differs from other known galactic ridge radiation distributions in that it shows a narrowly peaked maximum around the center. It can be characterized by an $\sim 12^\circ$ FWHM Gaussian central bulge plus a broad disk-like component. The only physical model based on plausibly associated galactic ridge distributions which can fit the observations well in longitude is the predicted galactic nova spheroid distribution, but scaled down by $\sim 2/3$ from the latitude-integrated model bulge longitude width. The best fit has no additional discrete source or broad-disk components, although small contributions are permitted by the data. Novae are thought to be progenitors of Type I supernovae, probable sources of positrons in the galaxy, so this correlation suggests that Type I supernovae are the primary source of the positrons producing the observed galactic ridge annihilation radiation.

Subject headings: galaxies: Milky Way – Galaxies: center – ISM: general – gamma rays: observations

1. INTRODUCTION

Positron-electron annihilation is an important tool in astrophysics because it provides unique signatures of the environment of the annihilation region, and indirectly of the source of the positrons. This radiation was first unambiguously detected through its 511 keV line radiation from sources outside the solar system in balloon observations of the galactic center by Johnson, Harnden

¹E. O. Hulburt Center for Space Research, Naval Research Laboratory, Washington, DC 20375-5352

²Department of Physics and Astronomy, Northwestern University, Evanston, IL 60208

& Haymes (1972). It has since been observed from the galactic center region by numerous balloon and satellite-borne experiments. Prior to the launch of the Compton Gamma Ray Observatory (*CGRO*), observations were made with broad-field-of-view instruments which were not able to resolve the spatial details of the galactic ridge positron annihilation radiation (e.g. Leventhal, MacCallum & Stang 1978, Riegler et al. 1981, Albernhe et al. 1981, Gardner et al. 1982, Paciesis et al. 1982, Share et al. 1988, Chapius et al. 1991, Gehrels et al. 1991, Teegarden et al. 1996). Extensive measurements of the 511 keV line intensity with OSSE (the Oriented Scintillation Spectrometer Experiment) on *CGRO* have shown no evidence for variability over a period of ~ 6 years (e.g. Purcell et al. 1993, 1994, 1997). Preliminary maps of the 511 keV line intensity around the galactic center using OSSE observations with multiple collimator orientation directions relative to the plane were best fit with a two-component model comprising a $\leq 8^\circ$ spheroidal bulge at the center and a narrow disk component having about 25% of the total observed intensity over the central radian (Purcell et al. 1994). Kinzer et al. (1996) used the ~ 5 times greater signal from both the 511 keV line and 3-photon positronium continuum intensities obtained from the subset of OSSE observations which had the long axis of the OSSE collimators aligned with the plane (to provide clean differential measurements of the ridge intensity) in a preliminary study of the positron annihilation distribution along the galactic ridge. These results indicated a somewhat broader $\sim 11^\circ$ FWHM central bulge together with evidence for a similar $\sim 20\%$ disk component.

Positrons can be produced by a number of mechanisms in our galaxy, including: cosmic ray interactions in the interstellar medium, pulsars, β^+ decay products from radioactive nuclei (e.g. ^{26}Al , ^{56}Ni , ^{44}Ti) produced by supernovae, novae, or Wolf-Rayet stars, and $\gamma\text{-}\gamma$ pair production in the vicinity of compact objects, e.g. an accreting black hole (see e.g. Stecker (1969), Ramaty & Lingenfelter (1994) for early and recent discussions). Both the sources and annihilation environments of the positrons will be reflected in the spatial distribution, spectral characteristics, and time history of the observed annihilation radiation. Measurements of the positron annihilation radiation thus provide a unique tool for both probing the energetic processes in the galaxy and for studying components of the interstellar medium.

The OSSE instrument on *CGRO* has the narrow collimation and offset background measurement capabilities needed to resolve the galactic ridge's spatial details. It also has the sensitivity needed to measure the spectra from this diffuse source with high statistical precision. The current work reports measurements of the latitude and longitude distributions of both the 511 keV line and the 3-photon positronium continuum components of the annihilation radiation along the inner galactic ridge using the limited subset of the OSSE observations which had the long axis of the collimator aligned with the galactic plane and which performed symmetrical background observations at $b^{II} \sim \pm 10^\circ$. In these, the background fields are minimally contaminated by emission from the extended galactic plane, and uncertainties in interpretations of the complex galactic plane continua are minimized. Preliminary results for the positron annihilation longitude distribution using a portion of these data have been reported (Kinzer et al. 1996). In the current work, corrections for a subtle dependence of the OSSE internal background on the angle of an

OSSE detector viewing direction relative to the spacecraft axis (Kurfess et al. 1997) has permitted an improved understanding of the underlying continua (Kinzer, Purcell, and Kurfess 1997), and hence has provided more accurate measurements of the positron annihilation components. The resulting increase by about a factor of 5 in the available positron annihilation signal provided by the three-photon positronium continuum component significantly enhances the ability to resolve spatial details along the galactic ridge relative to analyses using only the 511 keV line intensity.

2. OBSERVATION AND DATA ANALYSIS

The OSSE instrument comprises four identical and independently orientable NaI(Tl)-CsI(Na) phoswich spectrometers, each of which has an aperture of $\sim 3.8^\circ$ by 11.4° full-width at half-maximum (FWHM) at 0.511 MeV defined by a passive tungsten slat collimator. The positron-electron annihilation observations reported here were conducted and processed in the manner described in the OSSE instrument description paper of Johnson et al. (1993). A more detailed description of the data analysis procedures used in analysing the 50 keV to 10 MeV diffuse emission from the galactic ridge is given by Kinzer, Purcell, & Kurfess (1997).

Here we use only the subset of the OSSE observations of the inner galactic plane which had the long direction of the collimator approximately aligned with the plane (position angle of $\sim 90^\circ$). In these the four detectors were operated in a source/background chopping mode in which each detector alternately viewed the galactic ridge (over a fixed longitude region defined by the collimator aperture) for two minutes and, alternately, one of two background fields located roughly 10° on either side of the plane for two minutes. These observations provide differential measurements of the central galactic ridge emission relative to the residual intensities at $b^{II} = \pm 10^\circ$. Observations at six longitude positions satisfied these criteria and were also sufficiently deep to provide useful measurements or limits on the positron annihilation radiation. At the center, two separate observation sequences measuring the intensity as a function of latitude between $b^{II} = -3^\circ$ and $+3^\circ$ were performed in viewing period (VP) 5 and VP 16. Away from the center, useful measurements were only at $b^{II} = 0^\circ$. Table 1 gives observational details of the measurements used in the current analysis.

As shown by Kinzer, Purcell, and Kurfess (1997), after correction for a small scan-angle dependence in the internal detector background, the diffuse spectra from the galactic ridge can be well-represented by a four-component model comprising an annihilation radiation component (consisting of a narrow line centered at 511 keV and a three photon orthopositronium continuum - Ore & Powell, 1949), plus underlying soft and hard continua (see Fig. 1). The soft low-energy continuum component is best represented by an exponentially absorbed power-law, while the hard component can be represented either by a cosmic-ray interaction model (Skibo, 1993) or by a power-law with photon index ~ -1.75 which approximates this model over the 50 keV to 10 MeV range. Although the 511 keV line intensities reported here are roughly independent of the continuum model used, the positronium continuum component intensities are significantly

affected by the choices of continuum model. The above model, determined by Kinzer, Purcell, and Kurfess (1997) both to best represent individual measurements and to give consistent results for the 50 keV to 10 MeV spectra from deep observations along the ridge, is used in the current work. Similar conclusions for the continuum models were reached by Kinzer et al. (1997) in examining the effect of different continuum models on the positronium fraction values from observations of the inner galactic ridge.

3. EXPERIMENTAL RESULTS

3.1. Latitude Distribution at the Center

Similar series of measurements of the galactic ridge at the center were made in VP 5 and in VP 16, with useful observations at $l^{II} = 0^\circ$ for latitudes $b^{II} = 0^\circ$, $b^{II} = \pm 1.5^\circ$, and $b^{II} = \pm 3.0^\circ$, and brief (not useful in the current analyses) observations at $b^{II} = \pm 5.5^\circ$. The summed spectra from the two observations at $l^{II} = 0^\circ$ for $b^{II} = 0^\circ$, $b^{II} = |1.5^\circ|$, and $b^{II} = |3.0^\circ|$ are shown in Fig. 1. The decrease of the positron annihilation components intensities with latitude apparent in this figure is shown more quantitatively in Figs. 2a, 2b, and 2c which give intensities of the positronium continuum, the 511 keV line, and the sum of the two components, respectively, as a function of galactic latitude. The solid line in each figure is the Gaussian shape, as smoothed by the detector response function, which best fits the measured composite annihilation radiation distribution in Fig. 2c, normalized to the respective data points. Within the statistical precision of the measurements, the 511 keV line and the 3-photon continuum components have indistinguishable measured latitude distributions. Fig. 3 shows the total annihilation radiation obtained from similar fits to these data, but with symmetrical latitude observations summed for improved fitting statistics. The same Gaussian shape, convolved with the detector response, (solid line) fits these data well. Deconvolution of the 3.8° FWHM OSSE collimator response function in the scan direction from this best-fit detector-convolved curve gives an $\sim 4.4^\circ$ FWHM Gaussian shape for the galactic ridge around the center. This derived model shape for the galactic ridge is shown by the area-normalized dashed curve in Fig. 2c and in Fig. 3 where the intensities are normalized to enclose the same integral area as the respective best-fit detector-convolved curves. Note that the intensities in these figures are not corrected for deconvolution of the detector response in longitude (see below), so that the units are "relative". Because adequate measurements were not made at latitudes greater than 3° , these differential measurements do not rule out the presence of broader "wings" on the distribution, nor the presence of a more intense but much broader underlying component (e.g. Purcell et al. 1997). Effects of any broader distribution contaminating the background fields will be to decrease the measured intensities relative to the true values without changing the differential shape in latitude.

3.2. Longitude Distribution

As indicated in Table 1, measurements of the galactic ridge at $b^{II} = 0^\circ$ which meet the criteria of the current analyses were made at $l^{II} = 0^\circ$, $l^{II} = 10^\circ$, $l^{II} = 16^\circ$, $l^{II} = 25^\circ$, $l^{II} = 40^\circ$, and $l^{II} = 350^\circ$. Fig. 4a shows the fitted intensity values for the 3-photon positronium continuum as a function of galactic longitude for these observations obtained using the above 4-component model. Fig. 4b shows a similar distribution for the 511 keV component, and Fig. 4c shows the composite annihilation radiation distribution. In these plots, the latitude width of 4.4° measured near the center (Fig 3) is assumed at all longitudes in unfolding the intensity as a function of longitude. Because the four components follow at least two, and possibly more, different longitude distributions, a flat distribution in longitude has been assumed in unfolding the photon spectra from the observed count-rate spectra (see Kinzer, Purcell, and Kurfess 1997 for more details). With this approach, an estimate of the actual source distribution for a given component can be obtained by convolving the OSSE collimator response and an assumed source distribution model to obtain a best-fit to the observed (detector-smoothed) distribution. The 11.4° FWHM OSSE collimator angular response in the trans-scan direction smooths the input from a narrowly peaked source distribution three times as much as does the narrow collimator response in the scan direction (Figs. 2 and 3).

As has been suggested previously (Purcell et al. 1994, Kinzer et al. 1996), a simple two-component model, which includes a Gaussian shape for the central longitude bulge component and a broad (in longitude) disk-like component which follows the galactic ridge CO gas distribution (excluding the narrow central $\sim 3^\circ$ wide spike - Dame et al. 1987), can represent the data well. The solid line in Fig. 4c shows the best-fit of this composite model, convolved with the detector response, to the observed detector-smoothed total annihilation radiation distribution. The curves shown in Figs. 4a and 4b, which are simple normalizations of this fitted shape for the detector-smoothed intensities for the composite signal in Fig. 4c, provide acceptable fits to these measured component distributions as well. In Fig. 4c the input composite model is shown by the dashed curve, while the input model components are shown by the dotted line (central gaussian bulge) and the dashed-dotted line (CO disk), respectively. An $\sim 12^\circ$ FWHM Gaussian model gives a best fit for the bulge component. Although the Gaussian shape has no known physical basis, the assumed galactic CO disk model has the form expected from the annihilation of positrons produced in the decay of galactic ^{26}Al (e.g. Mahoney et al 1984, Share et al. 1985) which was observed recently by COMPTEL (Diehl et al. 1995) to roughly follow the galactic CO distribution. The best-fit intensity for this disk component is $\sim 20\%$ of the derived integral intensity between 50° and 310° longitude.

4. DISCUSSION

The current measurements provide a quantitative estimate of the distribution along the inner galactic ridge of both the 0.511 MeV line and the three-photon continuum components of the annihilation radiation. Within the statistical accuracy of these observations, the line and continuum components are distributed in longitude along the plane indistinguishably and symmetrically about the galactic center (Fig. 4). Near the galactic center the two components are within the statistical uncertainties of being distributed the same in latitude as well (Figs. 2). This is confirmed by the uniform values of the *observed* positronium fraction which were measured in all available pointing directions to be consistent with a value of ~ 1.0 over the galactic ridge, as reported by Kinzer et al. (1997).

The measured $\sim 4.4^\circ$ FWHM latitude distribution (Fig. 3) suggests a distribution correlated with the galactic disk, rather than with the galactic bulge. However, the differential measurement of the disk intensities relative to background fields at $b^{II} = \pm 10^\circ$ could hide a broader component. Measurements at larger latitudes with background fields further from the plane are needed to resolve this question. Note that this observed width for the positronium annihilation component is about a degree narrower than, but not inconsistent with, the width measured for the 50 to 600 keV continuum by Purcell et al. (1996) using independent OSSE measurements.

However, in longitude the observed annihilation radiation bulge component differs markedly from previously observed galactic ridge radiation distributions, and thus limits possible origins for the positron annihilation radiation component. The detector-smoothed distribution is sharply peaked toward the galactic center, implying an even sharper source distribution. Thus it is not likely to be associated with the much more broadly distributed atomic or molecular gas components of the ISM along the plane. For comparison, the annihilation bulge has a detector-deconvolved width of $\sim 12^\circ$ FWHM (Fig. 4c) as compared to $\sim 80^\circ$ FWHM for the CO distribution. This observed shape is too broad to be from a few discrete sources clustered at the center, and too narrow to come from distributions following the matter distribution in the inner galactic ridge, such as the CO, hot plasma, warm gas, or high-energy gamma-ray continuum distributions (e.g. Skibo, Ramaty, & Leventhal 1992). The observed symmetry about the center further suggests a population distribution rather than emission from a few bright objects.

The most likely candidates for producing the positrons are Type I supernovae, which can produce adequate amounts of ^{56}Ni and ^{44}Ti , which produce positrons in their decay chains, to explain the observations (e.g. Colgate, 1970; Chan & Lingenfelter, 1993). The accreting white-dwarf progenitors of Type I supernovae are associated with novae, so comparisons with nova distributions may provide clues to the validity of this origin for the longitude bulge component. Conversely, the measured annihilation radiation distribution can provide unique information about the rather uncertain distribution of supernovae (and by inference novae) in the Galaxy if it can be proven that they are the source of this radiation. Note that Leising and Clayton (1987) showed that classical novae cannot produce the required number of positrons to explain the observed

galactic ridge emission.

Although the nova distribution in the Galaxy is only poorly known due to obscuration, the nova distribution in the somewhat similar M31 (Andromeda) galaxy has been observed over the past 90 years. These results provide insights into the nova distribution in our Galaxy. Ciardullo et al. (1987) used their H_α nova observations and historical nova observations to show that the nova bulge distribution in M 31 is well-represented by the shape of bulge component of the optical light distribution. Further, they found that the nova distribution in M31 is dominated by novae in the galactic bulge, with relative densities $\rho_{bulge}/\rho_{disk} \geq 10$. Higdon and Fowler (1987) used these results, along with measurements and models in the Milky Way, to obtain both spheroidal and disk nova distribution models for the Galaxy.

Fig. 5 shows a best-fit of a 3 component distribution model, which included a discrete source at the center, a latitude-integrated version of the nova spheroid shape as suggested by Higdon and Fowler (1987), and a disk component following the CO galactic ridge distribution. In this fit, the predicted form of the rather uncertain nova spheroid distribution was scaled in width with a free parameter in the fit. An acceptable best fit ($\chi^2 \sim 1.1$ per degree of freedom) was obtained with a width ~ 0.66 times that of the predicted model, with no discrete source or broad disk contributions required. The one-sigma ($\chi^2 + 1$) limit on a discrete source contribution is $\sim 15\%$ of the total ridge emission from the central radian. Although the broad disk component is poorly constrained by the observations, the one-sigma limit on a broad disk contribution is $\sim 12\%$ of the observed flux over the central radian.

Higdon & Fowler (1987) also provided a disk nova distribution which is similar to a smoothed version of the CO distribution used in the above fits, and provides essentially similar fitted results when included as a free component in place of the CO distribution.

Given the large uncertainty in the predicted galactic nova distribution, the factor of 1/3 narrower distribution implied by the current observations is not unreasonable. The ability of this single-component distribution model to fit the observations with only a scaling in width gives strength to claims that this approximates the correct source distribution. Circumstantially, the observed annihilation radiation distribution along the galactic ridge much more closely resembles the center-peaked nova-spheroid distribution model than models for other plausibly related distributions (see, e.g. Skibo, Ramaty, and Leventhal 1992 for a discussion of possible distributions). However, as noted above, the narrow latitude distribution observed is not consistent with a truly spherical bulge distribution, but suggests a disk-flattened bulge distribution. The observed annihilation radiation distribution may be the best information available to determine the nova and supernova distributions, rather than the other way around.

If the poorly constrained disk component follows the assumed CO distribution model, acceptable fits using the Nova bulge model permit the broad disk to have sufficient intensity to account for the $\sim 8 - 18\%$ contribution to the total galactic center positron annihilation flux expected (Chan & Lingenfelter, 1993) from the observed distribution of ^{26}Al in the inner galaxy

(e.g. Diehl et al. 1995). Further, although contributions from a galactic center discrete source, such as that expected from the black-hole candidate 1E1740.7-2942, are not present in the best fit to the data, contributions of as much as 20% of the total flux from the central radian from one or more strong discrete sources near the center cannot be excluded. Inclusion of discrete-source contributions in the fits broadens the best-fit nova bulge shape, with a width of 1.0 times the Higdon and Fowler model width indicated at a 20% discrete source contribution.

Because of OSSE’s differential mode of measuring the galactic ridge intensities (symmetrical background fields $\sim 10^\circ$ from the plane are subtracted from the plane observations), the current measurements do not speak to any underlying broad-latitude disk or bulge components (e.g. Purcell et al. 1997).

The positron annihilation observations discussed here and the positronium fraction results discussed by Kinzer et al. (1997) provide a new understanding of the positron annihilation along the central galactic ridge. A cursory examination of Table 1 and Figs. 2 and 4 shows that the ability of the OSSE instrument to provide an accurate definition of the galactic ridge annihilation radiation emission has been barely tapped by the sparse and relatively shallow existing observations. The instrument is currently working at 100% of its original capability, and has a projected life of several more years. If deep (4 to 8 week) observations at closely spaced longitude and latitude directions along the ridge can be scheduled (with the long axis of the collimator aligned parallel to the plane), then the detailed spatial and spectral characteristics of the galactic ridge can be much better defined in the coming years.

We acknowledge helpful discussions with Mark Strickman, Jeff Skibo, Neil Johnson, & Greg Jung. This work was supported under NASA grant DPR S-10987C.

Dates	Viewing Period	Live Time ^a	Orientation ^b	Direction (l^I, b^I)
1991 July 12-26	5	4.5	90°	(0°, 0°)
	5	1.2	90°	(0°, −1.5°)
	5	1.2	90°	(0°, −3.0°)
	5	1.2	90°	(0°, 1.5°)
	5	1.2	90°	(0°, 3.0°)
1991 December 12-27	16	5.5	90°	(0°, 0°)
	16	1.2	90°	(0°, −1.5°)
	16	1.2	90°	(0°, −3.0°)
	16	1.2	90°	(0°, 1.5°)
	16	1.2	90°	(0°, 3.0°)
1991 August 15-22	7	1.2	90°	(25°, 0°)
1991 October 31-November 7	13	5.1	90°	(25°, 0°)
1992 February 6-20	20	4.8	90°	(40°, 0°)
1994 November 15-29	404	6.7	89°	(10°, 0°)
1994 December 20-January 3	407	4.5	82°	(350°, 0°)
1997 February 4-11	624	3.6	91°	(16°, 0°)
1997 June 10-17	620	4.5	92°	(16°, 0°)

Table 1: OSSE INNER GALACTIC RIDGE OBSERVATIONS

^aTotal live-times for background-subtracted and screened data in units of 10^5 seconds per single-detector equivalent on source.

^bGalactic position angle (angle relative to galactic north) of the long direction of the collimator.

REFERENCES

- Chan, K. & Lingenfelter, R. 1993, *ApJ*, 405, 614
- Chapuis, C. G. L., et al. 1991, in *Gamma-Ray Line Astrophysics*, ed. P. Durouchoux & N. Prantzos (New York:AIP), 52
- Ciardullo, R, Ford, H. C., James, D. N., Jacoby, G. H., & Shafter, A. W. 1987, *ApJ*, 318, 520
- Dame, T. et al. 1987, *ApJ*, 322, 706
- Diehl, R. et al. 1995, *A&A*, 298, 445
- Gardner, B. M., et al. 1982, in *The Galactic Center*, ed. G. R. Riegler & R. D. Blandford (New York:AIP), 144
- Gehrels, N., Barthelmy, B., Teegarden, B., Tueller, J., Leventhal, M., & MacCallum, C. 1991, *Ap. J.*, 375, L13
- Higdon, J. C. & Fowler, W. A. 1987, *ApJ*, 317, 710
- Johnson, W. N., Harnden, F. R., & Haymes, R. C. 1972, *ApJ*, 172, L1
- Johnson, W. N., Kinzer, R. L., Kurfess, J., Strickman, M., Purcell, W., Grabelsky, D., Ulmer, M., Hillis, D., Jung, G., & Cameron, R. 1993, *Ap. J. Suppl.*, 86, 693
- Kinzer, R. L., Purcell, W. R., Johnson, W. N., Kurfess, J., Jung, G. and Skibo, J. 1996, *Astron. Astrophys. Suppl.*, 120, 317
- Kinzer, R. L., Purcell, W. R., & Kurfess, J. D. 1997, *Ap J.*, (Submitted)
- Kinzer, R. L., Purcell, W. R., Skibo, J., Strickman, M., Johnson, N. & Kurfess, J. D. 1997, *Ap J.*, (In preparation)
- Kurfess, J. D., Kinzer, R. L., Purcell, W. R., & McNaron-Brown, K. 1997, in *The Fourth Compton Symposium*, eds. Dermer, C., & Kurfess, J. D. (AIP: New York), In Press
- Leising, M. D., & Clayton, D. D. 1987, *ApJ*, 323, 159
- Leventhal, M., MacCallum, C. J., & Stang, P. D. 1978, *ApJ*, 225, L11
- Mahoney, W., Ling, J., Wheaton, W., & Jacobson, A. 1984,
- Paciesas, W. S., Cline, T. L., Teegarden, B. J., Tueller, J., Durouchoux, P., & Hameury, J. M. 1982, *ApJ*, 260, L7
- Ore, A. & Powell, J. 1949, *Phys. Rev.*, 75, 1696
- Purcell, W., Grabelsky, D., Ulmer, P., Johnson, W., Kinzer, R., Kurfess, J., Strickman, M., & Jung, G. 1993, *Ap J.*, 413, L85.
- Purcell, W., et al. 1994, in *The 2nd Compton Symp.*, ed. C. Fichtel, N. Gehrels, & J. Norris (New York:AIP), 403
- Purcell, W. R., et al. 1996, *Astron. Astrophys. Suppl.*, 120, 389
- Purcell, W. R., et al. 1997, *Ap J.*, (submitted)

- Ramaty, R., & Lingenfelter, R. E. 1994, in *High Energy Astrophysics*, ed. J. Matthews (Singapore:World Scientific),
- Riegler, G. R., et al. 1981, *ApJ*, 248, L13
- Share, G. H., Kinzer, R. L., Kurfess, J. D., Forrest, D. J., Chupp,
Share, G. H., Kinzer, R. L., Kurfess, J. D., Messina, D. C., Purcell, W. R., Chupp, E. L., Forrest,
D. J., & Reppin, C. 1988, *ApJ*, 326, 717
- Skibo, J. G. 1993, Ph.D. Dissertation, University of Maryland.
- Skibo, J., Ramaty, R. & Leventhal, M. 1992, *ApJ*, 397, 135
- Stecker, F. W. 1969, *Ap Space Sci*, 3, 579
- Teegarden, B., et al. 1996, *Ap. J.*, 463, L75

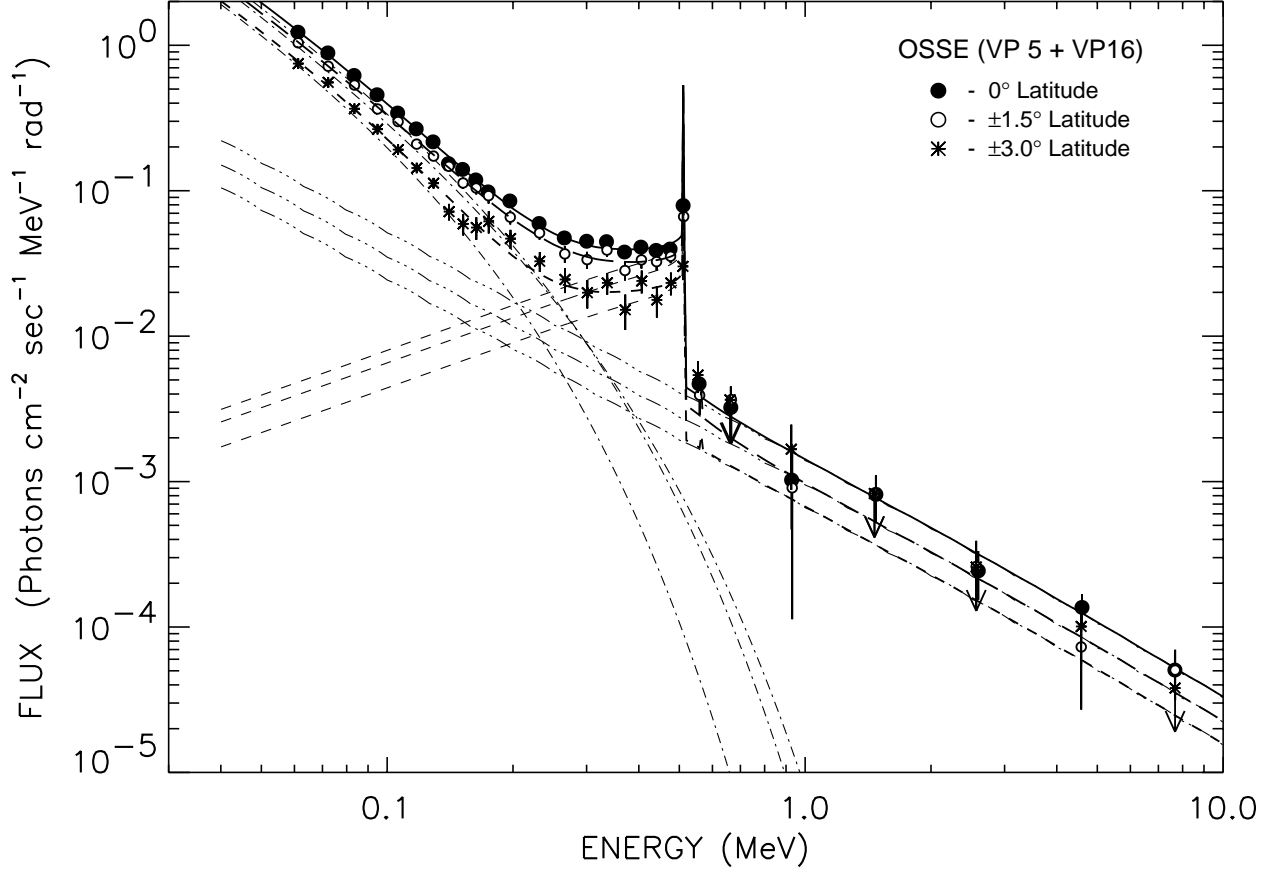
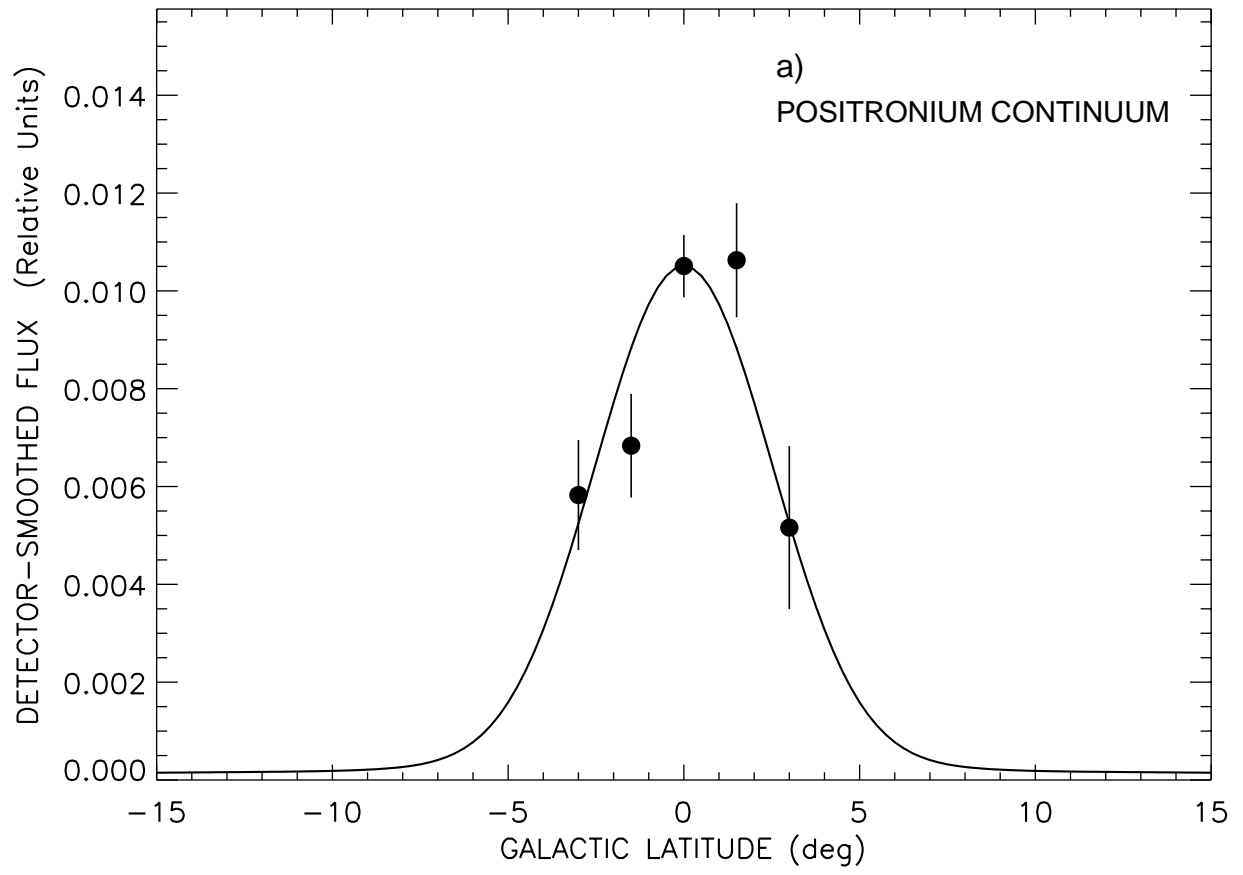
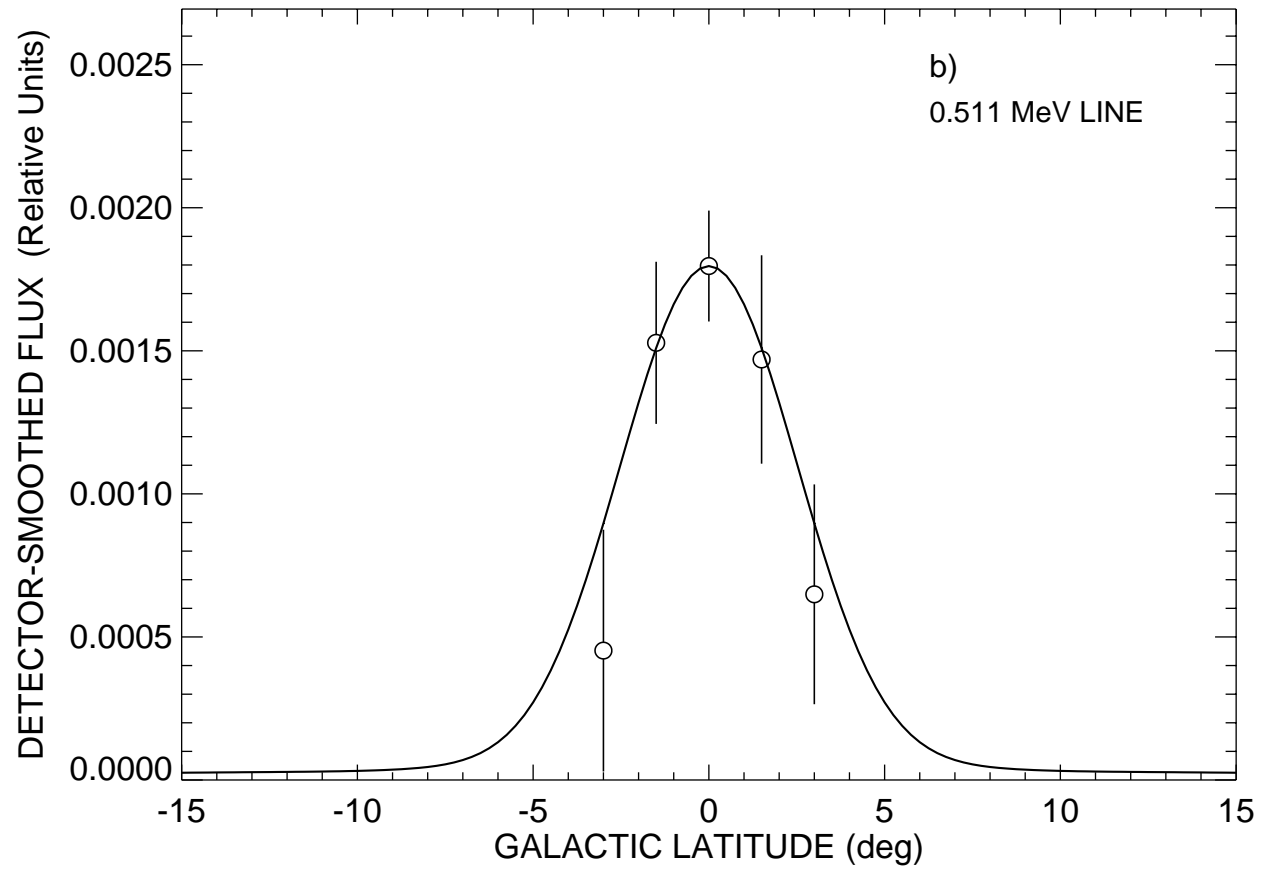


Fig. 1.— Spectra from the VP 5 and VP 16 galactic center pointings at 0° (solid line), 1.5° (long-dashed line), and 3° (dashed-dotted line) latitude. Positron annihilation components are indicated by light dashed lines, the low-energy continuum components are indicated by light dashed-dotted lines, and the high-energy (cosmic-ray induced) continuum components are shown by the dashed-triple-dotted lines.





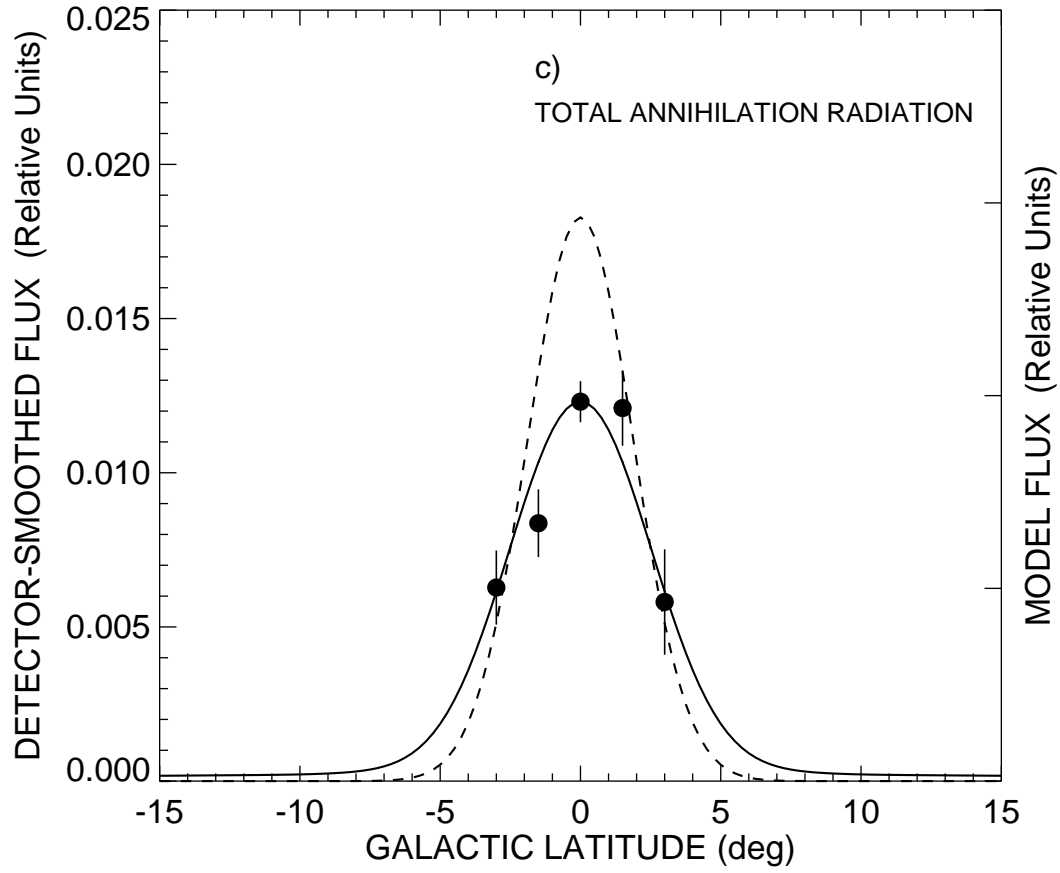


Fig. 2.— Latitude distribution of the three-photon continuum (a), 511 keV line (b), and the composite annihilation radiation intensities (c) at the galactic center. A 4.4 deg. FWHM gaussianmodel folded through the instrument response gives an acceptable fit to the data.

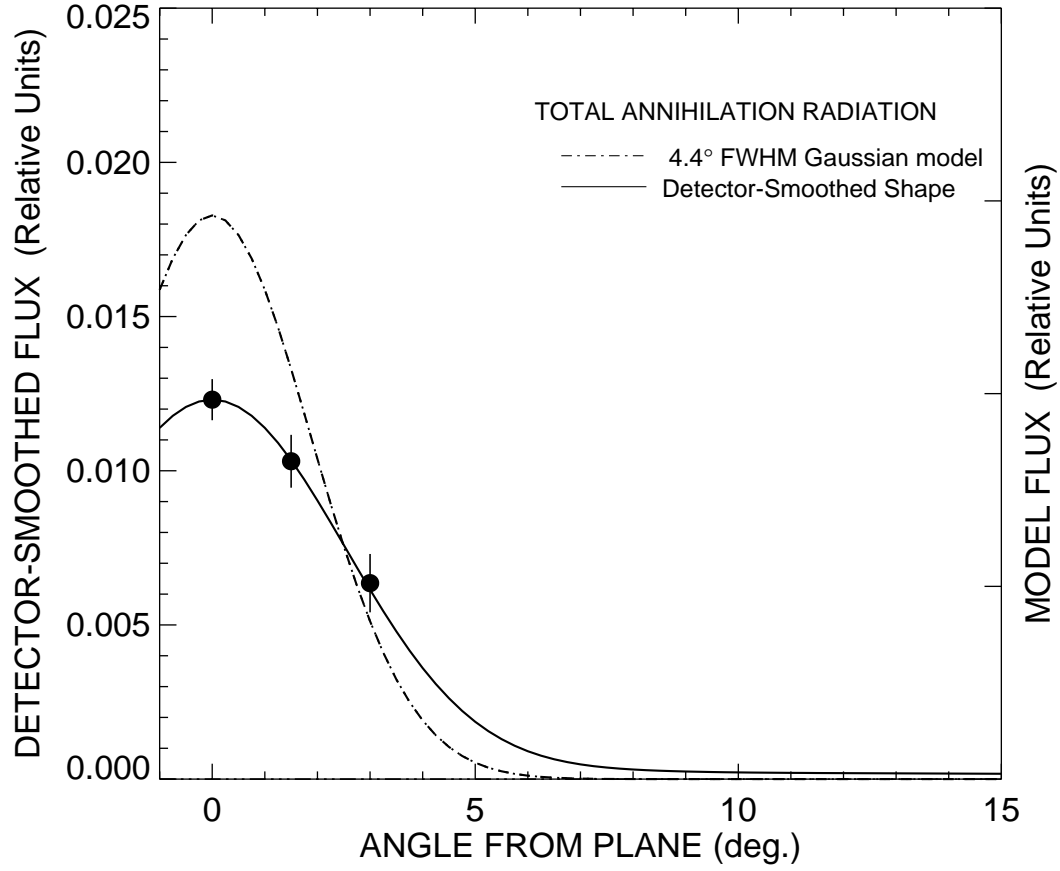
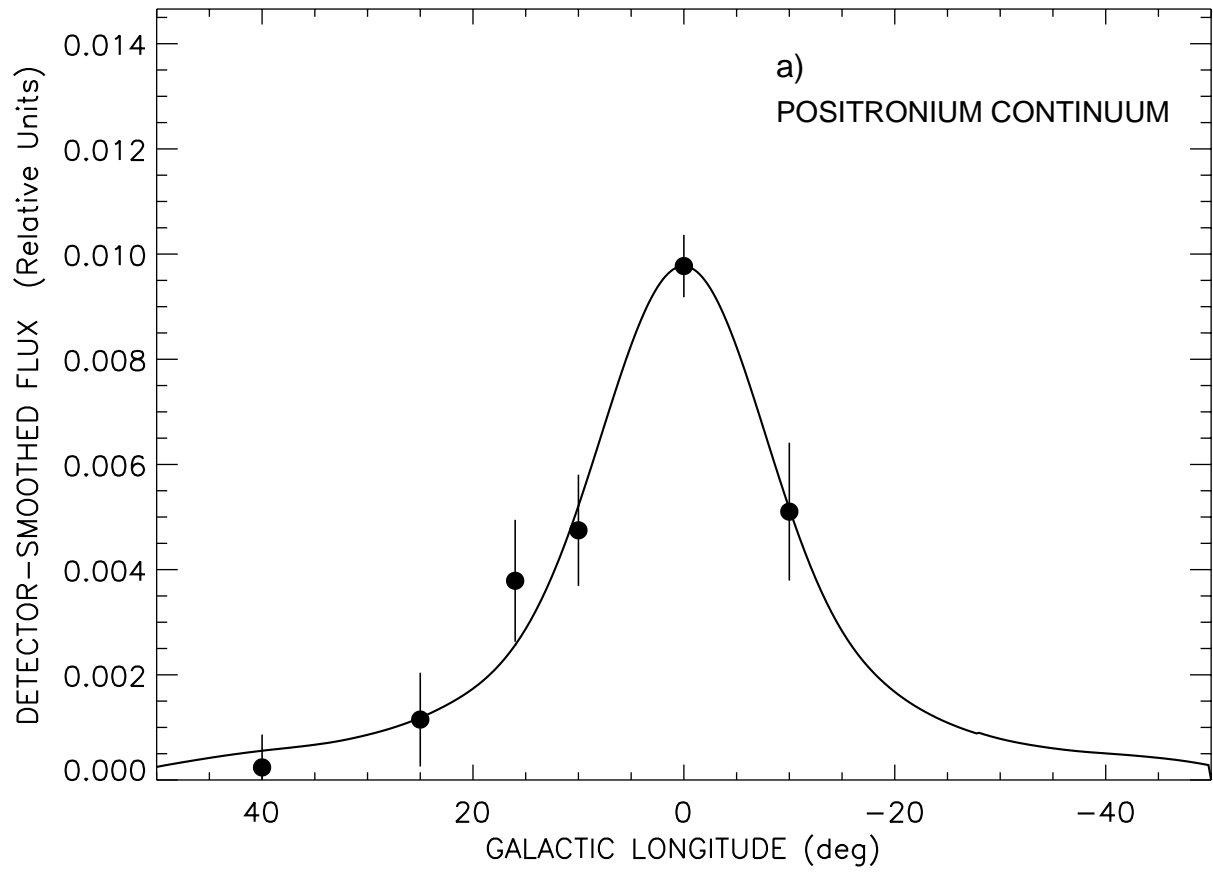
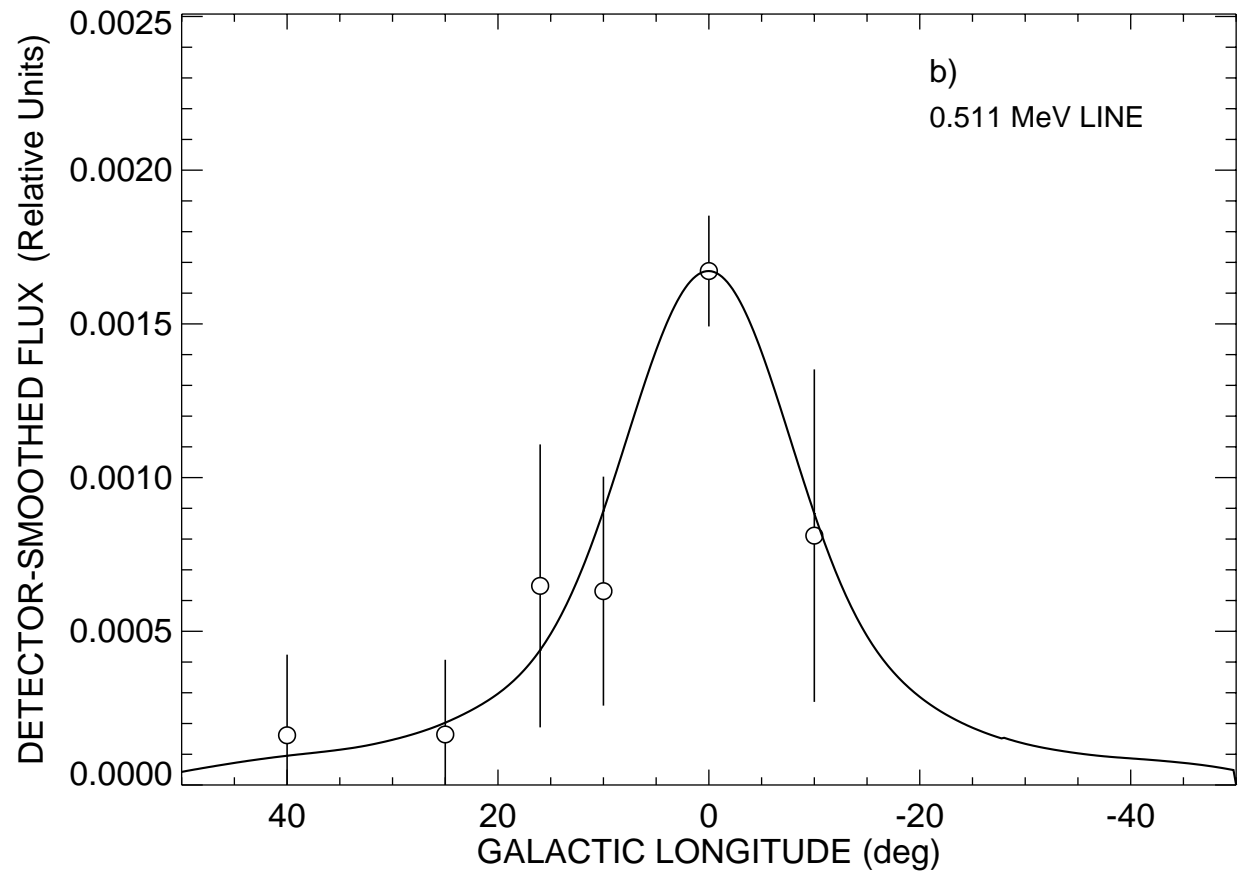


Fig. 3.— Latitude distribution of the composite annihilation radiation intensity at the galactic center with symmetrical latitudes summed for improved statistical precision. The same model used in Fig. 2 is shown.





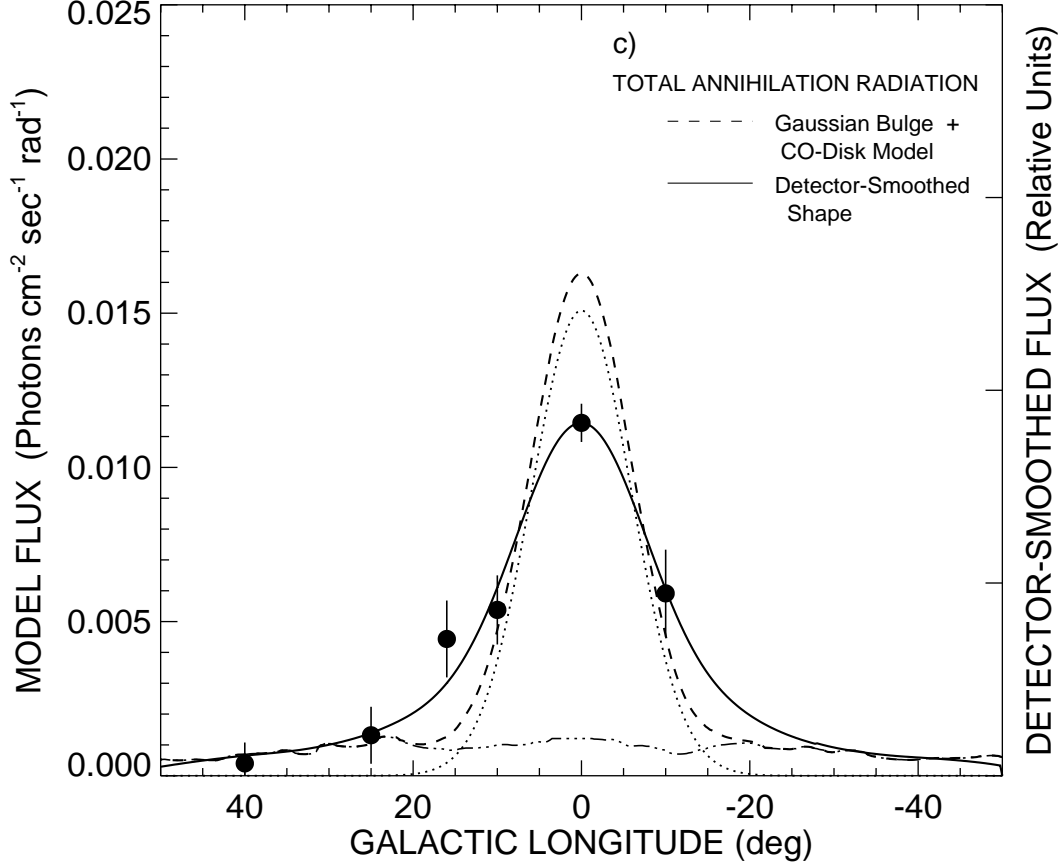


Fig. 4.— Longitude distribution of the observed annihilation radiation component intensities along the galactic ridge at $b^{II} = 0^\circ$. The 3-photon positronium continuum distribution is shown in a), the 511 keV distribution in b), and their sum in c). The best-fit of a gaussian bulge plus a CO disk model to the composite distribution in c), smoothed by the detector collimator response, is shown by the solid curve in each figure (curves are normalized to the respective data points). The dotted curve in c) is the input 12° FWHM model bulge shape, the dashed-triple-dotted curve is the CO disk component, and the dashed curve is the composite input model shape.

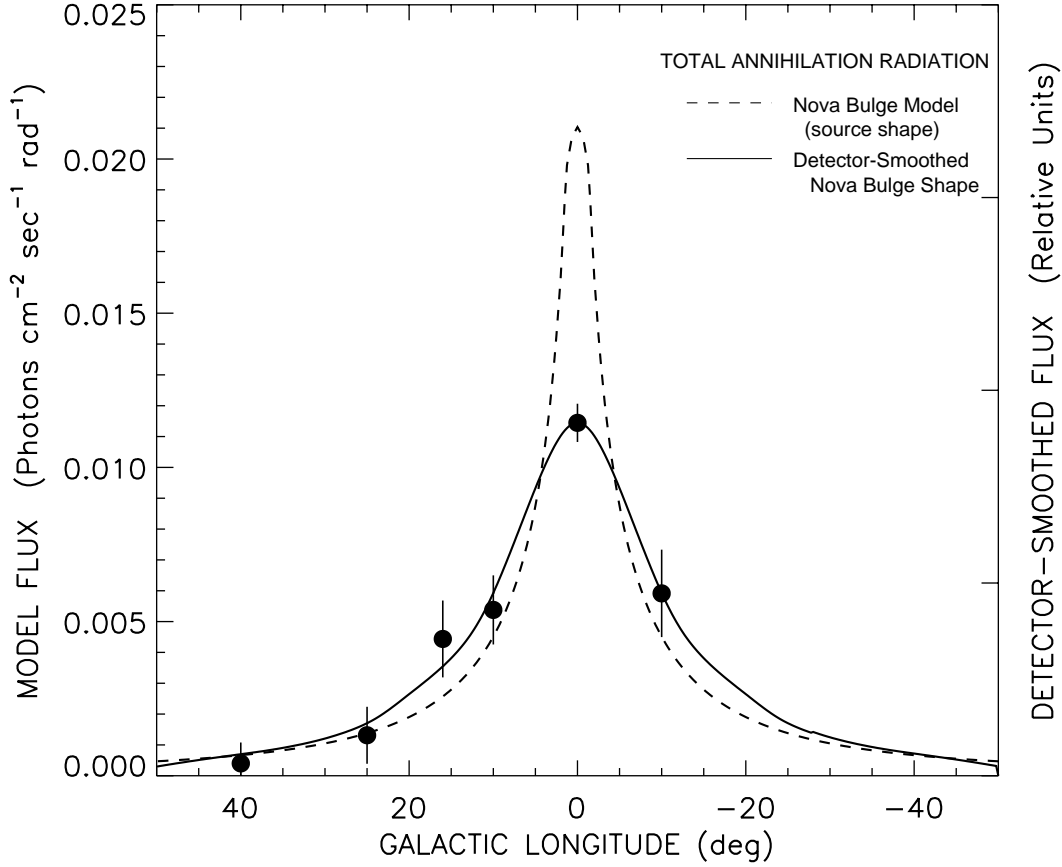


Fig. 5.— Longitude distribution of the composite annihilation radiation intensity along the galactic ridge at $l^{II} = 0^\circ$, fit with a Nova-bulge plus a CO-disk model convolved with the detector angular response. As in Fig. 3, a), b), and c) give the positronium continuum, the 511 keV line, and the composite distributions, respectively, with fits determined by the composite distribution only. No discrete source or broad disk contribution are needed in the best fit shown by the solid lines. The detector-deconvolved best-fit bulge model has a width about 2/3 that of the model of Higdon and Fowler. Flux units are given for the deconvolved model components.